Z. Phys. C – Particles and Fields 12, 333–343 (1982)

Zeitschrift für Physik C Particles and Fields

Gauge Vector Boson Pair Production at $\bar{p}p$ Collider Energies

M. Hellmund and Gisela Ranft
Sektion Physik, Karl-Marx-Universität, DDR-701 Leipzig, German Democratic Republic

Received 10 September 1981

Abstract. Within the standard $SU(2)\times U(1)$ model differential cross sections and angular distributions of all polarization states are studied for all channels of gauge vector boson pairs accessible in hadron hadron collisions, W^+W^-, Z^0Z^0, $Z\gamma$, ZW, γW. The zero in the unpolarized angular distribution of $q\bar{q}\to W\gamma$ reported theoretically by Mikaelian et al. [1] is confirmed. The origin of this zero is studied which was discovered by Brown, Mikaelian, Samuel, and Sahdev. None of the other channels exhibits a zero in the unpolarized angular distribution, but strong minima at $\cos\Theta=0$ are predicted for $q_i\bar{q}_j\to Z\gamma$ and $q_i\bar{q}_j\to ZW^+$. These are of different origin than the Mikaelian zero. Simple structure functions suggest that these minima are seen in $p\bar{p}$ collisions.

1. Introduction

With the $\bar{p}p$ collider going into operation in the near future it might be feasable to detect not only the long predicted intermediate vector bosons W and Z but also to measure pair production of gauge bosons. Although the cross section for pairs of gauge bosons in general is smaller by a factor of 10^{-3} as compared to the single vector boson production, it reaches about $4\cdot 10^{-36}\,\mathrm{cm}^2$ at $\sqrt{s}\simeq 200\,\mathrm{GeV}$ for $p\bar{p}\to W\gamma+X$ and at $\sqrt{s}\simeq 400\,\mathrm{GeV}$ for $p\bar{p}\to WZ+X$ [2]. With the foreseen luminosity this might result in a few times ten events in each channel within a year ($\sim 10^3$ h) of running time. These events would allow to study the coupling of three vector bosons which is typical for a non-abelian gauge theory. They could be signaled by the simultaneous decay of both vector bosons into leptons, thus giving four leptons in the final state. The angular distribution of the leptons in principle should indicate the polarization state of the decaying gauge boson. However, the leptonic decay will only comprise a few per cent of the events, since the largest decay mode of the vector bosons will be into two large $p_\perp$ jets each, thus giving a characteristic four-large $p_\perp$ jet signal.

As discovered by Mikaelian et al. [1] and Brown et al. [2], the reaction $q_i\bar{q}_j\to\gamma W$ should have a zero in the $q_i\bar{q}_j$ c.m.s. angular distribution, its position being determined by the quark charge Q_i according to

$$\cos\Theta=+(1+2Q_i) \tag{1}$$

independent of energy.

This would provide an interesting opportunity to measure the quark charge Q_i. The zero in the angular distribution only will appear when the triple vector boson coupling is gouverned by gauge theory; this demands the magnetic moment of the W to be

$$\mu_W=\frac{e}{2M_W}(1+k),\ k=1,\ \text{thus}\ \mu_W=\frac{e}{M_W}.$$

Although the $q\bar{q}$ cross section has to be folded with the structure functions, there is hope that in $p\bar{p}$ collisions the position of the zero in the angular distribution shows up as a dip, although smeared [2]. In pp collisions the folding with the structure functions might wash out the dip completely.

On the other hand, in e^+e^- collisions only the channels $e^+e^-\to W^+W^-$ and $\to Z^0Z^0$ are accessible. The cross section for fixed polarization states of the initial and final particles $e_L^-e_R^+$ and $e_R^-e_L^+\to V_{\lambda_1}V_{\lambda_2}$ have been extensively studied by Gaemers and Gounaris [3]. Not all cross sections with fixed initial and final polarizations develop a zero and if so, the zeroes of different polarization amplitudes are placed at different values in $\cos\Theta$. Moreover, these dips move in energy $\sqrt{s}$. The overal angular distribution for the unpolarized case, e.g. in $e^+e^-\to W^+W^-$, has a strong forward peak; it is caused by neutrino exchange in the $\hat{t}$ channel [4, 3] present for $e_L^-e_R^+\to W^+W^-$. The production of gauge boson pairs allows to study how the contributions of the various diagrams cooperate in

0170-9739/82/0012/0333/$02.20

order to produce a finite total cross section at very high energy, e.g. for $e^+e^- \to W^+W^-$ it is

$$\sigma \xrightarrow[s\to\infty]{} \frac{\pi\alpha^2}{2\sin^4\Theta_W}\frac{1}{s}\ln\frac{s}{M_W^2}$$

inspite of the cross section of the single contributing graphs growing like $\sim s$.

In an attempt to understand the occurance of the zero in the reaction $q_i\bar{q}_j \to W\gamma$ found by Mikaelian et al. [1, 2] we have computed the various polarization amplitudes for fixed quark and fixed gauge boson polarization in all channels which can be reached from the initial $q_i\bar{q}_j$ state with $q_i = u$ or d. These channels are

$$q_i\bar{q}_j \to W^-W^+ \quad (2a)$$
$$\to ZZ \quad (2b)$$
$$\to Z\gamma, \quad (2c)$$
$$d\bar{u} \to ZW^- \quad (2d)$$
$$\to \gamma W^-, \quad (2e)$$
$$u\bar{d} \to \gamma W^+ \quad (2f)$$
$$\to ZW^+. \quad (2g)$$

Three types of zeroes occur in the angular distributions of the polarization states

(i) a zero dependent on the quark charge but independent of energy and independent of the polarizations of the quarks and vector bosons (Brown, Mikaelian, Samuel, Sahdev zero BMSS-zero);
(ii) a zero at $\Theta = \pi/2$ occuring at some polarization states independent of energy;
(iii) zeroes moving in angle with energy occuring in some polarization states.

Only in the final state $\gamma W^\pm$ the zeroes of type (*i*) occur in all polarization states. This is due to the massless photon participating. This reaction selects only the initial $q_i^L\bar{q}_j^R$ polarization state.

In all other cases the zeroes of the one or other polarization amplitude (denoted by the polarization states (λ_1, λ_2) of the final vector bosons) are of type (*ii*) or (*iii*) and occur at different values of $\cos\Theta$, thus creating atmost a dip for the unpolarized angular distribution. The latter is the case for the reactions

$$q\bar{q} \to Z\gamma$$
$$\to ZW$$
$$\to ZZ,$$

for which $d\sigma/d\hat{t}$ at $\cos\Theta = 0$ is a factor 10^{-2}, 10^{-1} and 0.5, resp., smaller than near $\cos\Theta = \pm 1$. In the reactions $q\bar{q} \to Z\gamma$ and $\to ZZ$, however, the triple gauge boson coupling does not contribute. In $q\bar{q} \to Z\gamma$ this minimum is due to a zero at $\cos\Theta = 0$ of those polarization amplitudes which involve Z and γ polarized parallel to each other [amplitudes $(\lambda_1, \lambda_2) = (1,1)$, $(2,2)$, and $(3,3)$ and vanishing amplitudes for longitudinally polarized photons $(\lambda_1, \lambda_2) = (i, 3)$ $(i = 1, 2, 3)$]; the amplitude $(3,2)$ with longitudinal Z is very small. In $q\bar{q} \to ZZ$ it is mainly the non-vanishing of the Z's transverse degree of freedom which prevents the overall cross section from vanishing at $\cos\Theta = 0$.

In $q_i\bar{q}_j \to ZW$ the angular distribution at $\cos\Theta = 0$ is one order of magnitude smaller than near forward and backward direction. Similar to $q_i\bar{q}_j \to \gamma W$ this reaction selects one polarized initial state, $q_i^L\bar{q}_j^R$. In $q_i\bar{q}_j \to ZW$, $(\lambda_1, \lambda_2) = (3,3)$ and $(3,2) = (2,3)$ remain as only sizable amplitudes around $\cos\Theta \simeq 0$.

The minima in $Z\gamma$, ZZ, and ZW final states might be detectable experimentally in $p\bar{p}$ collisions.

In Sect. 2 we describe our calculation and give the expressions for the amplitudes with fixed initial and final polarization states.

In Sect. 3 we present the angular distributions for the reactions listed in (2) and discuss the origin of typical zeroes appearing in the polarization amplitudes.

2. Polarization Amplitudes for the Reaction $q_i\bar{q}_j \to V_1V_2$

We treat the production of vector boson pairs in lowest order. For initial u and d quarks we have listed the accessible reaction channels in (2); the appropriate exchange graphs are shown in Fig. 1. We notice that in the reactions $q\bar{q} \to Z^0Z^0$ and $Z^0\gamma$ the triple vector boson coupling does not appear.

2.1. Kinematics and Polarization States

Our calculation of the polarization amplitudes follows closely the method of Gaemers and Gounaris [3]. For completeness we repeat here the essential steps. We perform the calculation within the $SU(2) \times U(1)$ standard model (i.e. in the formulation of [3] we have $f_1 = 1$, $f_2 = 0$, $f_3 = 2$, $f_4 = \ldots = f_9 = 0$, $k_\gamma = k_Z = 1$, $\lambda_\gamma = \lambda_Z = 0$).

The Feynman rules are shown in Table 1. The $SU(2) \times U(1)$ couplings are collected in Table 2. The kinematics is similar to [3]. The notation is defined in Fig. 2. $E = \sqrt{\hat{s}}/2$ and $p_1(p_2)$ are energy and momentum of the quark (antiquark) in the $q\bar{q}$ c.m. frame. M_i, E_i, and q_i are the masses, energies and momenta of the outgoing vector bosons V_i $(i = 1, 2)$. The z axis is chosen along the momentum $\boldsymbol{p}_1$ of the incoming quark, (xz) is the reaction plane. The quark c.m.s. scattering angle Θ is the angle between $\boldsymbol{p}_1$ and $\boldsymbol{q}_1$. The x component of $\boldsymbol{q}_1$ is taken positive.

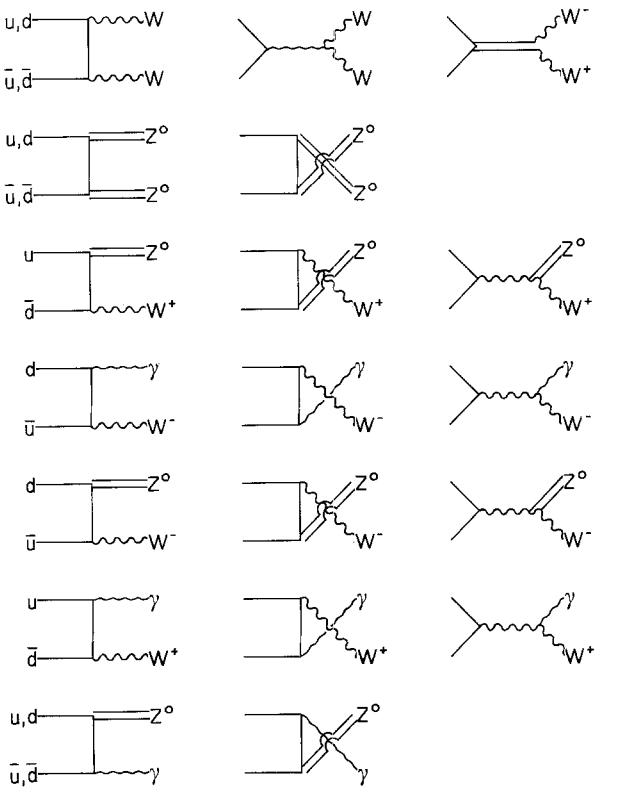

Fig. 1. The exchange graphs in lowest order contributing to the reactions (2)

There are three polarization states of a massive vector particle V; we label these by $\lambda = 1, 2, 3$

$\lambda = 1$ a polarization perpendicular to the momentum $\boldsymbol{q}$ within the reaction plane,

$\lambda = 2$ a polarization transverse to the reaction plane,

$\lambda = 3$ a longitudinal polarization.

The polarization wave functions are

– for vector boson V_1

$$\varepsilon^{\mu}(q_1, 1) = (0; \cos\Theta, 0, -\sin\Theta)$$
$$\varepsilon^{\mu}(q_1, 2) = (0; 0, 1, 0)$$
$$\varepsilon^{\mu}(q_1, 3) = (q_1; E_1 \sin\Theta, 0, E_1 \cos\Theta)/M_1$$

– for vector boson V_2 (3)

$$\varepsilon^{\mu}(q_2, 1) = (0; -\cos\Theta, 0, \sin\Theta)$$
$$\varepsilon^{\mu}(q_2, 2) = (0; 0, 1, 0)$$
$$\varepsilon^{\mu}(q_2, 3) = (q_2; -E_2 \sin\Theta, 0, -E_2 \cos\Theta)/M_2 .$$

The spin projection operators for the quark (anti-quark) are

$$q^s = \tfrac{1}{2}(1 + s\gamma_5)q \qquad s = \pm 1 . \tag{4}$$
$$\bar{q}^s = \tfrac{1}{2}(1 - s\gamma_5)\bar{q}$$

We often use the notation q^L and q^R etc. defined by

$$q^{s=-1} = q^L; \quad q^{s=+1} = q^R$$
$$\bar{q}^{s=-1} = \bar{q}^R; \quad \bar{q}^{s=+1} = \bar{q}^L . \tag{5}$$

The differential cross sections for fixed polarizations are

$$\frac{d\sigma^{L(R)}_{\lambda_1\lambda_2}}{d\hat{t}} = \frac{1}{16\pi\hat{s}^2}\left|\sum_{i=1}^{3} F^{L(R)}_{i\lambda_1\lambda_2}\right|^2 . \tag{6}$$

$F^{L(R)}_{i\lambda_1\lambda_2}$ are the amplitudes related to the three graphs shown in Fig. 2a–c.

Table 1. The Feynman rules $SU(2) \times U(1)$ gauge theory

q, q̄, A_μ	$-ieg^{q\bar{q}\gamma}\gamma_\mu$
q, q̄, V_μ	$-ie\{\gamma_\mu(1-\gamma_5)g_L^{Vq\bar{q}} + \gamma_\mu(1+\gamma_5)g_R^{Vq\bar{q}}\}$
$W^-_{\alpha_i}(q_1)$, $A_{\mu_i}(p)$, $W^+_{\beta_j}(q_2)$	$ie\{(q_2-q_1)_\mu g_{\alpha\beta} + (p_\beta g_{\mu\alpha} - p_\alpha g_{\mu\beta})\} \equiv ieU^{\gamma}_{\mu\alpha\beta}$
$W^-_{\alpha_i}(q_1)$, $Z^0_{\mu_i}(p)$, $W^+_{\beta_j}(q_2)$	$\varepsilon_{\alpha\beta\mu} ie\, g^{ZWW}\{2p_\beta g_{\mu\alpha} - 2p_\alpha g_{\mu\beta} + (q_2-q_1)_\mu g_{\alpha\beta}\}$ $\equiv ie\, g^{ZWW}\, U^{Z}_{\mu\alpha\beta}$

Table 2. The couplings involved in the calculation. Couplings to quark distinguish between left handed (q^L) and right handed (q^R) quarks ($t_u^3=\frac{1}{2}$, $t_d^3=-\frac{1}{2}$, $Q_u=\frac{2}{3}$, $Q_d=-\frac{1}{3}$, $\cos\theta_c=1$)

q_i, $\bar{q}_i$, $A_{i\mu}$	$g_R^{\gamma q\bar{q}}=g_L^{\gamma q\bar{q}}=\frac{1}{2}Q_q\equiv g^{\gamma q}$	$g^{\gamma u}=\frac{1}{3}$ $g^{\gamma d}=-\frac{1}{6}$
q_i, $\bar{q}_j$, $W_{i\mu}$	$g_L^{Wq_i\bar{q}_j}=g^{W\bar{q}_iq_j}=\frac{1}{2\sqrt{2}\sin\Theta_W}\equiv g_L^{Wq}$ $g_R^{Wq_i\bar{q}_j}=g_R^{W\bar{q}_iq_j}=0$	$g_L^{Wu}=g_L^{Wd}=\frac{1}{2\sqrt{2}\sin\Theta_W}$ $g_R^{Wu}=g_R^{Wd}=0$
q_i, $\bar{q}_i$, $Z^0_{i\mu}$	$g_L^{Zq\bar{q}}=\frac{t_q^3-Q_q\sin^2\Theta_W}{\sin 2\Theta_W}\equiv g_L^{Zq}$ $g_R^{Zq\bar{q}}=-\frac{Q_q\sin^2\Theta_W}{\sin 2\Theta_W}\equiv g_R^{Zq}$	$g_L^{Zu}=\frac{\frac{1}{2}-\frac{2}{3}\sin^2\Theta_W}{\sin 2\Theta_W}$ $g_L^{Zd}=\frac{-\frac{1}{2}+\frac{1}{3}\sin^2\Theta_W}{\sin 2\Theta_W}$ $g_R^{Zu}=\frac{-\frac{2}{3}\sin^2\Theta_W}{\sin 2\Theta_W}$ $g_R^{Zd}=\frac{\frac{1}{3}\sin^2\Theta_W}{\sin 2\Theta_W}$
W^1_μ, W^2_ν, Z^0_ρ	$g^{ZWW}=\cot\Theta_W$	
W^1_μ, W^2_ν, A_ρ	$g^{ZWW}=1$	

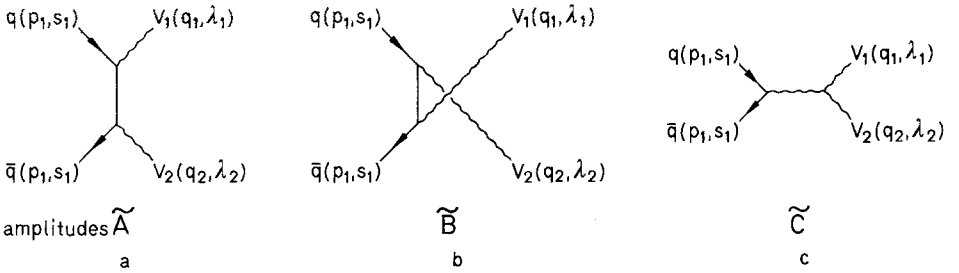

Fig. 2a–c. The lowest order graphs for gauge vector boson pair production and the notation and kinematics used

The angular cross section for definite polarizations is

$$\frac{d\sigma^{L(R)}_{\lambda_1\lambda_2}}{d\Omega}=\frac{|\boldsymbol{q}|\hat{s}}{4\pi E}\frac{d\sigma^{L(R)}_{\lambda_1\lambda_2}}{d\hat{t}}=\frac{|\boldsymbol{q}|}{E}\frac{\left|\sum_{i=1}^{3}F^{L(R)}_{i\lambda_1\lambda_2}\right|^2}{64\pi^2\hat{s}} \tag{7}$$

with $|\boldsymbol{q}|$ being the c.m.s. momentum of V_1 and $E=\frac{\sqrt{\hat{s}}}{2}$.

2.2. *The Method of Calculation*

To the reaction $q\bar{q}\to V_1+V_2$ contribute quark exchange in the $\hat{t}$ and $\hat{u}$ channels as well as vector boson exchange in the $\hat{s}$ channel. The appropriate graphs are shown in Fig. 2. The polarization amplitudes for the reaction

$$q^{s_1}\bar{q}^{s_2}\to V_{\lambda_1}V_{\lambda_2} \tag{8}$$

with the definite polarizations λ_1 and λ_2 of the two final vector bosons and the fixed polarizations s_1 and

s_2 of the initial q and $\bar{q}$ have the form

$$F^{s_1 s_2}_{\lambda_1 \lambda_2} = g \bar{v}(p_2, s_2) \Gamma^{\alpha\beta} u(p_1, s_1) \varepsilon_\alpha(q_1, \lambda_1) \varepsilon_\beta(q_2, \lambda_2). \tag{9}$$

g contains the coupling constants to be read off from Table 2. Following Gaemers and Gounaris in the use of Bjorken's method [5] the use of a transverse unit vector $n^\mu = (0; 0, 1, 0)$ inserted as $\not{n}$ between the quark and antiquark spinors

$$\xi = \bar{u}(p_1, s_1) \not{n} v(p_2, s_2) \tag{10}$$

gives automatically the projection into the only two initial spin states of physical significance in zero quark mass kinematics

$$\xi = \begin{cases} 2iE & \text{if } s_1 = -1, s_2 = +1 \\ & \text{or } s_1 = +1, s_2 = -1 \\ 0 & \text{otherwise.} \end{cases} \tag{11}$$

Multiplying the amplitude (9) by ξ introduces a trace already in the amplitude

$$F^{s_1 s_2}_{\lambda_1 \lambda_2} = g \frac{1}{2iE} \cdot \mathrm{Tr}\{\tfrac{1}{2}(1 + s_1\gamma_5) \not{p}_1 \not{n} \tfrac{1}{2}(1 - s_2\gamma_5) \not{p}_2 \Gamma^{\alpha\beta}\} \cdot \varepsilon_\alpha(q_1, \lambda_1) \varepsilon_\beta(q_2, \lambda_2). \tag{12}$$

of the propagator. We have

$$A^{L(R)}_{\lambda_1 \lambda_2}(\Theta) = \frac{1}{2iE} \mathrm{Tr}\{\tfrac{1}{2}(1_{(\mp)}\gamma_5) \not{p}_1 \not{n} \tfrac{1}{2}(1^{-}_{(+)}\gamma_5) \not{p}_2 \cdot \not{\varepsilon}_2(q_2, \lambda_2)(1_{(\mp)}\gamma_5)(\not{p}_1 - \not{q}_1) \cdot \not{\varepsilon}_1(q_1, \lambda_1)(1_{(\mp)}\gamma_5)\}. \tag{13}$$

Similarly, for the $\hat{u}$ channel exchange graph (Fig. 2b) quantities $B^{L(R)}_{\lambda_1 \lambda_2}$ are defined; they are related to $A^{L(R)}_{\lambda_1 \lambda_2}$ by reflection of the angle Θ around π and interchange of λ_1 and λ_2

$$B^{L(R)}_{\lambda_1 \lambda_2}(\Theta) = A^{L(R)}_{\lambda_2 \lambda_1}(\Theta + \pi) \tag{14}$$

and

$$M_1, E_1 \leftrightarrow M_2, E_2.$$

We denote by $C^{L(R)}_{\lambda_1 \lambda_2}$ the spin dependent part of the amplitude belonging to Fig. 2c. The functions A, B, C depend on Θ, $E = \sqrt{\hat{s}}/2$, $|q| = q$, M_i and E_i $(i = 1, 2)$.

We present A and C as matrices $A_{\lambda_1 \lambda_2}$ and $C_{\lambda_1 \lambda_2}$ separately for the two polarization states L and R of the initial quark antiquark system.

We have

$$\frac{1}{8E} A^L = \begin{pmatrix} \sin\Theta(|q| - 2E\cos\Theta) & i\sin\Theta(E_1 - 2E) & \frac{1}{M_2}(-2EE_2\sin^2\Theta + q^2 - 2|q|E\cos\Theta + E_1E_2) \\ iE_1\sin\Theta & -|q|\sin\Theta & -\frac{i}{M_2}(E_1E_2\cos\Theta + q^2\cos\Theta - 2E|q|) \\ \frac{1}{M_1}(2EE_1\cos^2\Theta - M_1^2 - 2E|q|\cos\Theta) & -\frac{i}{M_1}(2E|q| - q^2\cos\Theta - 2EE_1\cos\Theta + E_1^2\cos\Theta) & \frac{\sin\Theta}{M_1M_2}(-2EE_2|q| + |q|^3 + 2E_1E_2E\cos\Theta) \end{pmatrix} \tag{15}$$

and

$$\tfrac{1}{8} C^L = \begin{pmatrix} -|q|\sin\Theta & 0 & \frac{1}{M_2} 2|q|E\cos\Theta \\ 0 & |q|\sin\Theta & -i\frac{1}{M_2} 2|q|E \\ -\frac{1}{M_1} 2E|q|\cos\Theta & i\frac{1}{M_1} 2|q|E & \frac{|q|\sin\Theta}{M_1M_2}(E_1^2 + E_2^2 + E_1E_2 - q^2) \end{pmatrix}. \tag{16}$$

We use the label L for the initial state $q^L\bar{q}^R(s_1 = -1, s_2 = +1)$ and R for $q^R\bar{q}^L(s_1 = +1, s_2 = -1)$. The spin dependent part of the $\hat{t}$ channel exchange amplitude (Fig. 2a) is denoted by $A^{L(R)}_{\lambda_1 \lambda_2}(\Theta)$. It differs from the amplitude by the missing of the coupling constants and

For V_1 or V_2 being a photon, the amplitudes involving its longitudinal degree of freedom have to vanish for general reasons, $M_\gamma = 0$ does not cause a divergence.

The spin dependent quantities $A^R_{\lambda_1 \lambda_2}$ and $C^R_{\lambda_1 \lambda_2}$ for the initial state $q^R\bar{q}^L$ differ from (15) and (16) atmost by

a sign. They are

$$A^R_{\lambda_1\lambda_2}(\Theta)=(-1)^{\lambda_1+\lambda_2+1}A^L_{\lambda_1\lambda_2}(\Theta), \tag{17}$$

$$C^R_{\lambda_1\lambda_2}(\Theta)=(-1)^{\lambda_1+\lambda_2+1}C^L_{\lambda_1\lambda_2}(\Theta). \tag{18}$$

From (16) we note that the triple vector boson amplitude $C_{\lambda_1\lambda_2}$ vanishes for V_1 polarized perpendicular to its momentum $\boldsymbol{q}_1$ within the scattering plane and V_2 polarized transverse to the scattering plane and vice versa. In the following formulae

$$\mathscr{R}=\frac{\hat{s}-M_i^2}{(\hat{s}-M_i^2)^2+\Gamma_i^2M_i^2} \qquad i=1,2 \tag{19}$$

is the Breit-Wigner curve for the vector boson $V_i(i=1,2)$. Using A, B, and C the contributions to the polarization amplitudes $F^{L(R)}_{\lambda_1\lambda_2}$ Eq. (9) are (Q_q is the quark charge)

– for reaction $q_i\bar{q}_i\to W^+W^-$:

$$\begin{aligned}
\tilde{A}^L_{\lambda_1\lambda_2}&=(g^{q\bar{q}W}_L)^2A^L_{\lambda_1\lambda_2}\frac{1}{\hat{t}}\\
\tilde{B}^L_{\lambda_1\lambda_2}&=0\\
\tilde{C}^L_{\lambda_1\lambda_2}&=g^{\gamma q\bar{q}}g^{\gamma WW}\frac{1}{\hat{s}}(C^L_{\lambda_1\lambda_2})_{\gamma\,\text{exch.}}\\
&\quad+g^{Zq\bar{q}}_Lg^{ZWW}\mathscr{R}(C^L_{\lambda_1\lambda_2})_{Z^0\,\text{exch.}}\\
\tilde{A}^R_{\lambda_1\lambda_2}&=\tilde{B}^R_{\lambda_1\lambda_2}=0\\
\tilde{C}^R_{\lambda_1\lambda_2}&=g^{\gamma q\bar{q}}g^{\gamma WW}\frac{1}{\hat{s}}(C^R_{\lambda_1\lambda_2})_{\gamma\,\text{exch.}}\\
&\quad+g^{Zq\bar{q}}_Rg^{ZWW}\mathscr{R}(C^R_{\lambda_1\lambda_2})_{Z\,\text{exch.}}.
\end{aligned}$$

The label "γ exchange" and "Z exchange" denote the $\hat{s}$ channel exchanges of γ and Z, resp., see Fig. 1.

– for reaction $q\bar{q}\to Z^0Z^0$:

$$\begin{aligned}
\tilde{A}^{L(R)}_{\lambda_1\lambda_2}&=(g^{Zq\bar{q}}_{L(R)})^2\frac{1}{\hat{t}}A^{L(R)}_{\lambda_1\lambda_2}\\
\tilde{B}^{L(R)}_{\lambda_1\lambda_2}&=(g^{Zq\bar{q}}_{L(R)})^2\frac{1}{\hat{u}}A^{L(R)}_{\lambda_2\lambda_1}\\
\tilde{C}^{L(R)}_{\lambda_1\lambda_2}&=0
\end{aligned} \tag{21}$$

– for reaction $q_i\bar{q}_j\to Z^0W$ $i\neq j$

$$\begin{aligned}
\tilde{A}^L_{\lambda_1\lambda_2}&=g^{Zq_i}_Lg^{Wq_i}_L\frac{1}{\hat{t}}A^L_{\lambda_1\lambda_2}\\
\tilde{B}^L_{\lambda_1\lambda_2}&=g^{Zq_i}_Lg^{Wq_i}_L\frac{1}{\hat{u}}A^L_{\lambda_2\lambda_1}\\
\tilde{C}^L_{\lambda_1\lambda_2}&=g^{Wq_i}_Lg^{WZ}_L\mathscr{R}C^L_{\lambda_1\lambda_2}\\
\tilde{A}^R_{\lambda_1\lambda_2}&=\tilde{B}^R_{\lambda_1\lambda_2}=\tilde{C}^R_{\lambda_1\lambda_2}=0
\end{aligned} \tag{22}$$

– for reaction $q_i\bar{q}_j\to\gamma W^{\pm}$, $i\neq j$

$$\begin{aligned}
\tilde{A}^L_{\lambda_1\lambda_2}&=g^{\gamma q_i}_Lg^{Wq}_L\frac{1}{\hat{t}}A^L_{\lambda_1\lambda_2}\\
\tilde{B}^L_{\lambda_1\lambda_2}&=g^{\gamma q_i}_Lg^{Wq}_L\frac{1}{\hat{t}}A^L_{\lambda_1\lambda_2}\\
\tilde{C}^L_{\lambda_1\lambda_2}&=g^{Wq}_Lg^{\gamma WW}_L\mathscr{R}C^L_{\lambda_1\lambda_2}\\
\tilde{A}^R_{\lambda_1\lambda_2}&=\tilde{B}^R_{\lambda_1\lambda_2}=\tilde{C}^R_{\lambda_1\lambda_2}=0
\end{aligned} \tag{23}$$

– for reaction $q_i\bar{q}_i\to Z^0\gamma$

$$\begin{aligned}
\tilde{A}^L_{\lambda_1\lambda_2}&=g^{Zq_i}_Lg^{\gamma q_i}\frac{1}{\hat{t}}A^L_{\lambda_1\lambda_2}\\
\tilde{B}^L_{\lambda_1\lambda_2}&=g^{Zq_i}_Lg^{\gamma q_i}\frac{1}{\hat{u}}A^L_{\lambda_2\lambda_1}\\
\tilde{C}^L_{\lambda_1\lambda_2}&=0\\
\tilde{A}^R_{\lambda_1\lambda_2}&=g^{Zq_i}_Rg^{\gamma q_i}\frac{1}{\hat{t}}A^R_{\lambda_1\lambda_2}\\
\tilde{B}^R_{\lambda_1\lambda_2}&=g^{Zq_i}_Rg^{\gamma q_i}\frac{1}{\hat{u}}A^R_{\lambda_2\lambda_1}\\
\tilde{C}^R_{\lambda_1\lambda_2}&=0.
\end{aligned} \tag{24}$$

The coupling constants are given in Table 2. The differential cross sections for the reactions listed in (2a–g) with definite polarizations of the initial $q\bar{q}$ system and of the final gauge boson pair V_1V_2 are

$$\frac{d\sigma^{L(R)}_{\lambda_1\lambda_2}}{d\hat{t}}=\frac{e^4}{16\pi s^2}|F^{L(R)}_{\lambda_1\lambda_2}(\hat{s},\hat{t},\hat{u};\Theta_W)|^2. \tag{25}$$

The amplitude

$$F^{L(R)}_{\lambda_1\lambda_2}=\tilde{A}^{L(R)}_{\lambda_1\lambda_2}+\tilde{B}^{L(R)}_{\lambda_1\lambda_2}+\tilde{C}^{L(R)}_{\lambda_1\lambda_2}$$

follows for each process (2) from (20) to (24).

The interference terms are taken into account in the numerical evaluation; they are not exposed here in their analytical form.

3. Results and Discussion of the Origin of Zeroes and Minima in the Angular Distribution

3.1. The Reactions $q\bar{q}\to V_1V_2$

In Figures 3–7 we show the differential cross section $d^{R(L)}_{\lambda_1\lambda_2}/d\hat{t}$ as function of $\cos\Theta$ of the $q\bar{q}$ c.m.s. angle Θ for fixed initial (R or L) and final (λ_1,λ_2) polarizations of the reactions

$q_i\bar{q}_j\to\gamma W$ (Fig. 3),

$q_i\bar{q}_j\to Z^0\gamma$ (Fig. 4),

$q_i\bar{q}_j\to Z^0W$ (Fig. 5),

$q_i\bar{q}_i\to WW$ (Fig. 6),

$q_i\bar{q}_i\to Z^0Z^0$ (Fig. 7).

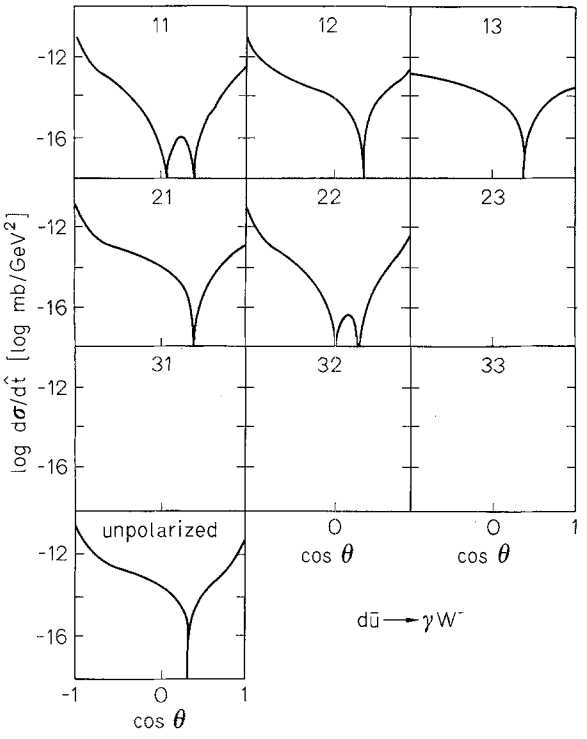

Fig. 3. The differential cross section $\frac{d\sigma}{d\hat{t}}$ for the reaction $d_L\bar{u}_R \to \gamma_{\lambda_1} W^-_{\lambda_2}$ as function of $\cos\Theta$ and its contributions from the various polarization states λ_1, λ_2 ($\lambda_1, \lambda_2 = 1, 2, 3$ as indicated on each single plot) and the case of unpolarized bosons but polarized initial quarks at $\sqrt{\hat{s}}/2 = 100\,\text{GeV}$

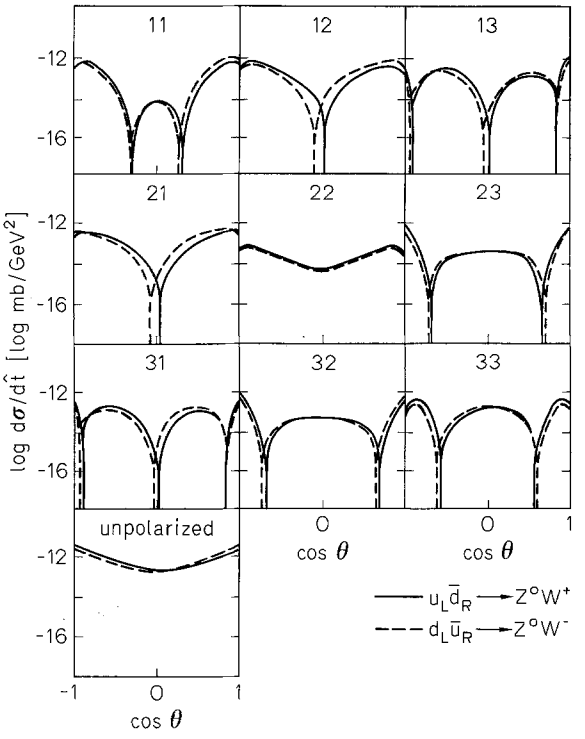

Fig. 5. As Fig. 3 but for $u_L\bar{d}_R \to Z^0W^+$ (——) and $d_L\bar{u}_R \to Z^0W^-$ (– – –)

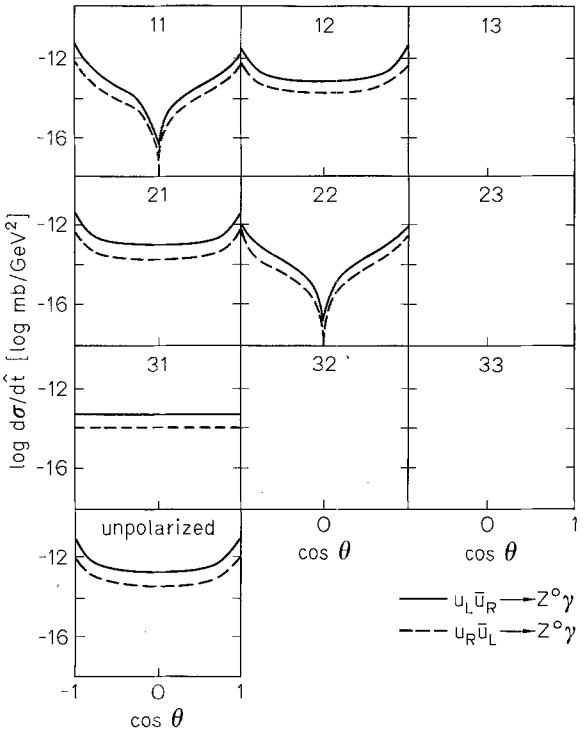

Fig. 4. As Fig. 3 but for $u_L\bar{u}_R \to Z\gamma$ (——) and $u_R\bar{u}_L \to Z\gamma$ (– – –).

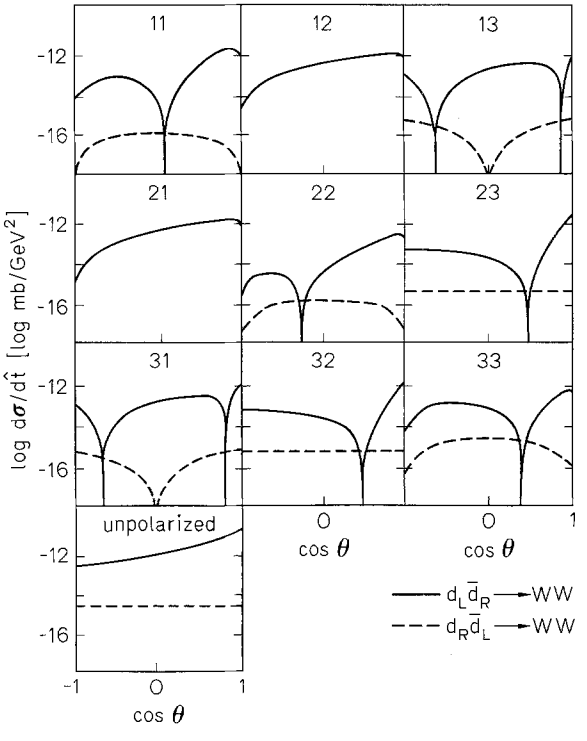

Fig. 6. As Fig. 3 but for $d_L\bar{d}_R \to W^-W^+$ (——) and $d_R\bar{d}_L \to W^-W^+$ (– – –)

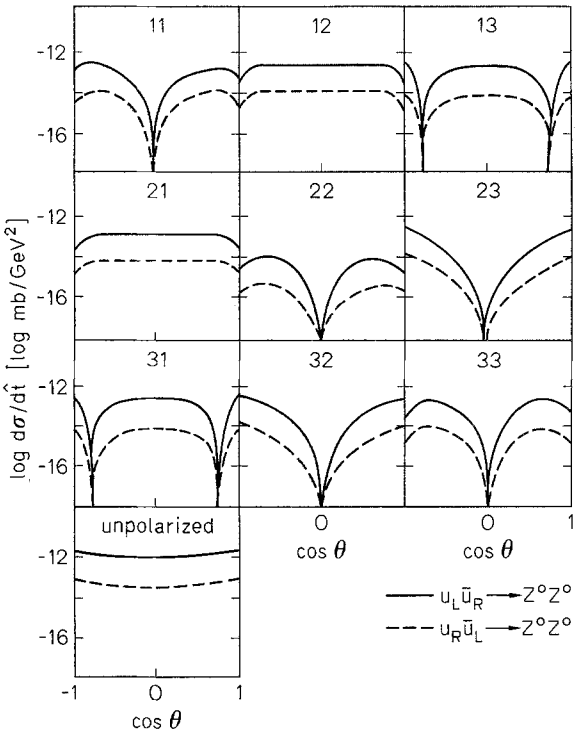

Fig. 7. As Fig. 3 but for $u_L\bar{u}_R \to Z^0Z^0$ (——) and $u_R\bar{u}_L \to Z^0Z^0$ (---)

We note:

The *zero in the unpolarized cross section appears only in the final state* $\gamma W^{\pm}$. In this reaction, the factor $(1+2Q_{q_i})$ is an overall factor for all polarization states (λ_1, λ_2) of V_1 and V_2. This was noted in an elegant way by Goebel et al. [6] and by Zhu Dongpei [7] and related to the group structure. This factorization is a consequence of gauge invariance, kinematics and dynamics; it relies on the participation of one massless gauge field. The W coupling selects only one initial polarization state $(q_L\bar{q}_R)$ through which the reaction may proceed. The relevant amplitude is $(i \neq j$; the polarization labels λ_1 and λ_2 are suppressed)

$$F^L = g_L^{Wq_i\bar{q}_j}\left[g^{\gamma q_i\bar{q}_i}\frac{A^L}{\hat{t}} + g^{\gamma q_j q_j}\frac{B^L}{\hat{u}} + g^{\gamma WW}\mathscr{R}_W C^L\right]. \tag{26}$$

E.g. for $d\bar{u} \to \gamma W^-$ this reads

$$F^L = \frac{1}{2\sqrt{2}\sin\Theta_W}\left(\tfrac{1}{2}Q_d\frac{A^L}{\hat{t}} + \tfrac{1}{2}Q_u\frac{B^L}{\hat{u}} + \mathscr{R}_W C^L\right). \tag{27}$$

It is seen to vanish at

$$\cos\Theta = -(1+2Q_d) = +1/3 \tag{1}$$

for any λ_1, λ_2 from the explicit forms A^L, B^L, and C^L according to (14)–(16), resp., and from use of energy momentum conservation in the form $\hat{s}+\hat{t}+\hat{u} = M_W^2$ (where the width $\Gamma_W \simeq 0$, for this check here). For $u\bar{d} \to \gamma W^+$ the zero occurs for all polarizations at

$$\cos\Theta = -(1-2Q_u) = -1/3.$$

In the reaction $q\bar{q} \to \gamma W$ the $(\lambda_1, \lambda_2) = (3, i)$ amplitudes $(i = 1, 2, 3)$ vanish identically due to $M_\gamma = 0$. The cross section for (2, 3) is below 10^{-20}. Due to $\Theta = 90°$ kinematics the polarization amplitudes (1, 1) and (2, 2) have a further zero at $\cos\Theta = 0$; this type of zero is discussed in connection to reaction $q_i\bar{q}_i \to Z^0\gamma$. Figure 4 shows the reaction $q_i\bar{q}_i \to Z\gamma$. Here both polarization states of the quarks contribute, $q^L\bar{q}^R$ and $q^R\bar{q}^L$; their angular distributions are proportional to each other by a factor

$$(g_L^{Zq_i}g_L^{\gamma q_i}/g_R^{Zq_i}g_R^{\gamma q_i})^2.$$

The absence of the triple gauge boson coupling prevents occurance of a BMSS zero. There is however a minimum in the unpolarized angular distribution; at $\cos\Theta = 0$ the cross section is over a factor 100 smaller than near $\cos\Theta = \pm 1$. This minimum is due to a zero of the polarization amplitudes (1, 1) and (2, 2) at $\cos\Theta = 0$; it is caused by $\Theta = 90°$ kinematics and the relations (14) between $B_{\lambda_1\lambda_2}$ and $A_{\lambda_2\lambda_1}$; it is independent of the quark charge and of $\hat{s}$. The amplitudes $(i, 3)$ $(i = 1, 2, 3)$ vanish identically since they would involve a longitudinal photon. The amplitude (3, 2) with a longitudinally polarized Z is very small $(< 10^{-20})$. The reaction $d\bar{d} \to Z\gamma$ behaves similar and is not plotted here.

A minimum of $\sim 10^{-1}$ at $\cos\Theta = 0$ as compared to $\cos\Theta \simeq \pm 1$ is found in reaction $u_L\bar{d}_R \to Z^0W^+$ (Fig. 5 continuous line). The W coupling discriminates against the initial state $u_R\bar{d}_L$. The amplitudes $(1, 2) = (2, 1)$ and $(1, 3) = (3, 1)$ have a zero near $\Theta \simeq 90°$ similar to the one discussed in connection with reaction $q\bar{q} \to Z^0\gamma$; the triple boson amplitudes $C_{13}^L \simeq C_{31}^L$ vanish at $\Theta = 90°$ and the amplitudes A_{13}^L and B_{13}^L would vanish for equal masses $M_1 \simeq M_2$. Moreover, the amplitudes (1, 1) and (2, 2) are small around $\Theta \simeq 90°$; the main contribution is due to scattering into the (3, 3) amplitude (having both, W and Z longitudinally polarized) and (3, 2) and (2, 3) amplitudes. The reaction $d_L\bar{u}_R \to Z^0W^-$ (broken line) does not differ much from $u_L\bar{d}_R \to Z^0W^+$, in polarization state (2, 2) they are identical. Especially these two channels leading to $Z^0W^{\pm}$ production show a very rich structure which combines the forward-backward peaking of the fermion exchange graphs with many zeroes of most of the polarization amplitudes. Figure 6 shows $u_L\bar{u}_R \to WW$ (continuous line); the reaction $d_L\bar{d}_R \to WW$ looks very similar. The forward peak is caused by the $\hat{t}$ channel quark exchance, the absence of the $\hat{u}$ channel graph prevents a backward peak. All polarization states but $(1, 2) = (2, 1)$

have zeroes. Less structure is shown in $u_R\bar{u}_L \to W^+W^-$ (Fig. 6 broken line) where only the amplitude $(1,3) = (3,1)$ vanishes at $\Theta = 90°$. Since this reaction receives contributions from two triple-boson couplings (γ and Z^0 exchange) these tend to smear each others effects to produce isotropy.

Moreover, due to the absence of the $\hat{u}$ channel exchange graph and massive kinematics the BMSS zero cannot develop. The $(1,2) = (2,1)$ cross section vanishes for $u_R\bar{u}_L$ since W does not couple. Comparing with $e^+e^- \to W^+W^-$ as given in [3] we find many similarities. The reaction $u_L\bar{u}_R \to Z^0Z^0$ is shown in Fig. 7 (continuous line). Compared with $u_R\bar{u}_L \to Z^0Z^0$ shown in Fig. 7 (broken line), $u_L\bar{u}_R \to Z^0Z^0$ is favoured by more than one order of magnitude, as expected. The reaction $d\bar{d} \to Z^0Z^0$ behaves similar but is smaller by one order of magnitude. The reaction $q\bar{q} \to ZZ$ does not involve the triple boson coupling. The amplitudes $(1,1)$, $(2,2)$, $(3,3)$, and $(2,3) = (3,2)$ produce at $\cos\Theta = 0$ a zero through $\Theta = 90°$ kinematics and the relation (14). The contributions from $(1,2) = (2,1)$ and $(1,3) = (3,1)$ fill in this zero, leaving only a minimum of a factor $\sim 1/2$ between $\cos\Theta = 0$ and near ± 1. We remark that compared with $u_L\bar{u}_R \to Z^0\gamma$ in Fig. 4 here also the longitudinal degrees of freedom [amplitudes $(2,3) = (3,2)$ and $(3,3)$] are excited; they develop a zero at $\cos\Theta = 0$. We note that the cross sections for $q_L\bar{q}_R \to ZZ$ are bigger by a factor of $(g_L^{Zq}/g_R^{Zq})^4$ than those of $q_R\bar{q}_L \to ZZ$.

Comparing with $e^+e^- \to Z^0Z^0$ given in [3] we find a rather similar structure here.

Some of the dips move with energy, as shown in Fig. 8 for $d_L\bar{u}_R \to Z^0W^-$ for $\sqrt{\hat{s}}/2 = 100\,\text{GeV}$ (continuous line) and $\sqrt{\hat{s}}/2 = 200\,\text{GeV}$ (dashed-dotted line), as already demonstrated by Gaemers and Gounaris [3] for e^+e^-. Contrarely to those, the BMSS dips (related to the quark charge) and the $\Theta = 90°$ dips remain fixed in energy.

In Fig. 9a–d we show the unpolarized angular distributions for $u_L\bar{u}_R \to ZZ$, $u_R\bar{u}_L \to ZZ$, $u_L\bar{d}_R \to ZW^+$ and $d_L\bar{u}_R \to Z^0W^-$ in a linear scale (note the differences in scale for each of these diagrams).

3.2. The Reaction $p\bar{p} \to V_1V_2$

To compare with experiments the cross sections for $q\bar{q}$ scattering have to be folded with the structure functions of q and $\bar{q}$ in p and $\bar{p}$. To find a rough estimate we use only valence structure functions as derived from quark counting rules. They are for u and d quarks in the unpolarized proton

$$\mathscr{F}_u^p = N_u(1-x)^3/\sqrt{x} \qquad N_u = 70/32, \tag{27}$$

$$\mathscr{F}_d^p = N_d(1-x)^4/\sqrt{x} \qquad N_d = 315/256, \tag{28}$$

and similar for $\bar{u}$ and $\bar{d}$ antiquarks in $\bar{p}$.

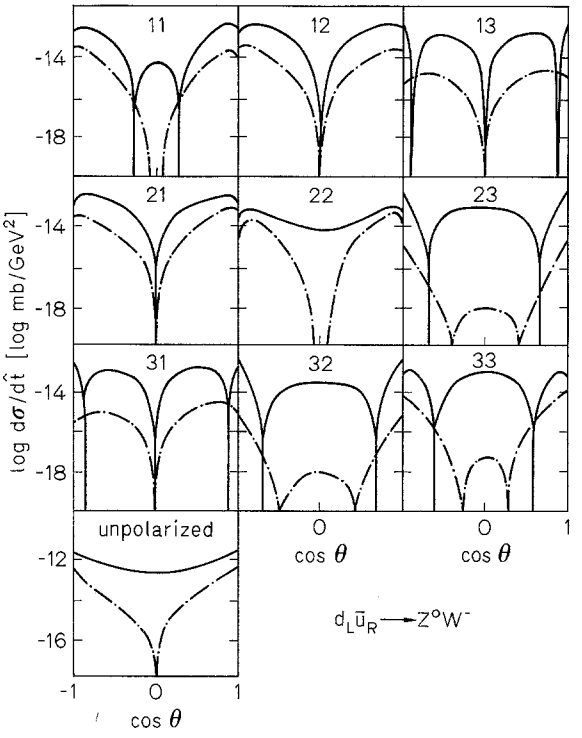

Fig. 8. The energy dependence of $\frac{d\sigma}{d\hat{t}}$ as function of $\cos\Theta$ for $d_L\bar{u}_R \to Z^0W^-$ $\sqrt{\hat{s}}/2 = 100\,\text{GeV}$ (——) and $\sqrt{\hat{s}}/2 = 200\,\text{GeV}$ (–·–·–) for the polarization states (λ_1, λ_2) of the vector bosons ($\lambda_1, \lambda_2 = 1, 2, 3$ as indicated on the single graphs) and for unpolarized vector boson pairs

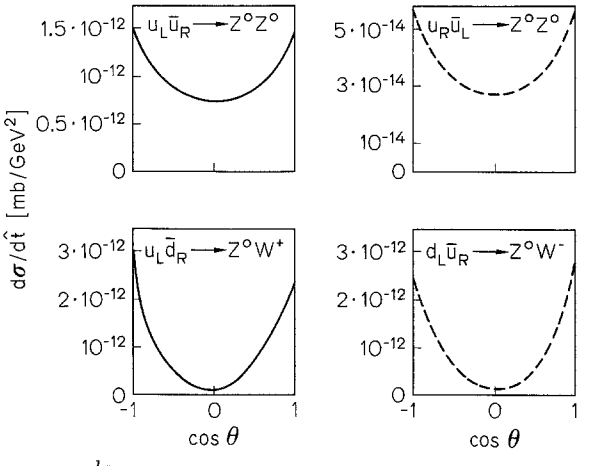

Fig. 9. $\frac{d\sigma}{d\hat{t}}$ as function of $\cos\Theta$ for the reactions $u_L\bar{u}_R \to ZZ$, $u_Ru_L \to ZZ$, $u_L\bar{d}_R \to ZW^+$ and $\bar{d}_L\bar{u}_R \to ZW^-$ for unpolarized vector bosons as plotted in Figs. 7 and 5 but here in a linear scale. (Note the differences in scale for the various subgraphs)

The factors N_u and N_d normalize to $p = uud$. We obtain the polarized distributions according to the $SU(6)$ model of Kaur [9] as used in [10]

$$\begin{aligned} u^-(x) &= \tfrac{1}{2}\mathscr{F}_d^p \qquad u^+(x) = \mathscr{F}_u^p - \tfrac{1}{3}\mathscr{F}_d^p \\ d^-(x) &= \tfrac{2}{3}\mathscr{F}_d^p \qquad d^+(x) = \tfrac{1}{3}\mathscr{F}_d^p . \end{aligned} \tag{29}$$

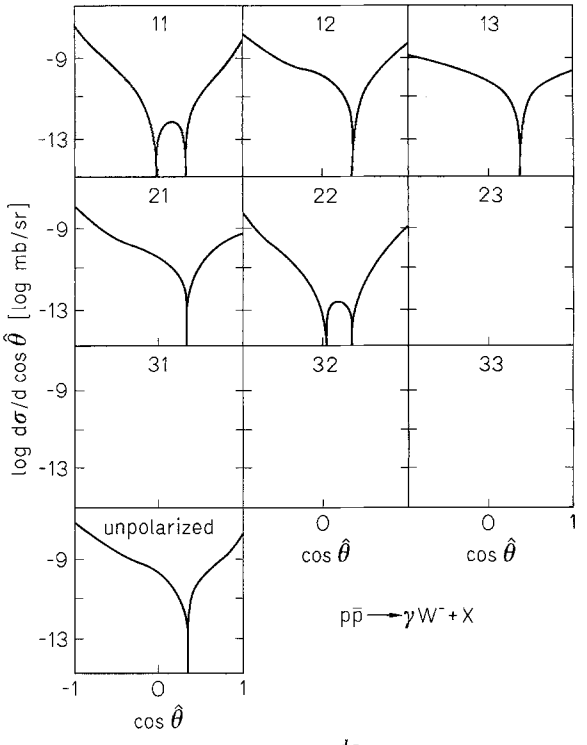

Fig. 10. The angular distribution $\frac{d\sigma}{d\cos\Theta}$ of the reaction $p\bar{p}\to\gamma W^-$ for all polarization states of the final vector bosons ($\lambda_1, \lambda_2 = 1, 2, 3$ as indicated on the subgraphs) but unpolarized initial state as well as the unpolarized final state at $\sqrt{s}/2 = 450\,\text{GeV}$

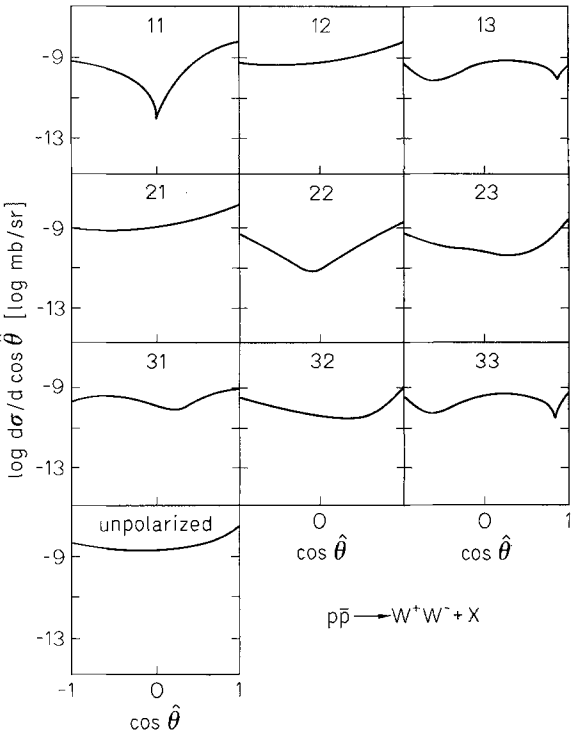

Fig. 11. As Fig. 10, but for $p\bar{p}\to W^+W^-$

Here u^+, d^+ (u^-, d^-) indicate the u and d quark distributions polarized parallel (antiparallel) to the proton polarization.

For our rough estimate all Q^2 dependence is neglected. Moreover, we neglect all transverse motion of quarks (which would introduce a further smearing).

To obtain unpolarized $p\bar{p}$ scattering we sum over all polarization states of the initial p and $\bar{p}$ ($i, j = 1, 2$) and over the polarizations R and L of q in p and $\bar{q}$ in $\bar{p}$. The angular distributions in the $p\bar{p}$ c.m.s. are ($\hat{\Theta}$ is the angle between the incoming proton and the produced vector boson V_1)

$$\frac{d\sigma}{d\cos\hat{\Theta}} = \tfrac{1}{3}\int_{M^2/s}^{1} dx_1 \int_{M^2/sx_1}^{1} \mathscr{J} \sum_{i,j=1,2} \left[F_{q_R}^{p_i}(x_1) F_{\bar{q}_L}^{\bar{p}_j}(x_2) \frac{d\sigma^R}{d\hat{t}} + F_{q_L}^{p_i}(x_1) F_{\bar{q}_R}^{\bar{p}_j}(x_2) \frac{d\sigma^L}{d\hat{t}} \right] \tag{30}$$

and

$$\mathscr{J} = \tfrac{1}{2}\sqrt{[\hat{s}-(M_1+M_2)^2][\hat{s}-(M_1-M_2)^2]}\,.$$

In the unpolarized case this formula coïncides with the one of [8].

Our results for reactions $p\bar{p}\to\gamma W^-$ and $p\bar{p}\to W^+W^-$ are shown in Figs. 10 and 11 for unpolarized initial states but all polarization states of the vector bosons as well as unpolarized final state. Due to our use of the valence structure functions only, we find a close similarity to the $q\bar{q}$ scattering; this is seen in comparing Fig. 10 with Fig. 3, both giving the final state γW^-. Due to the W^- coupling only to left handed quarks q_L, only one initial polarization state ($d_L\bar{u}_R$) contributes and the BMSS zero remaines in the unpolarized final state also for $p\bar{p}$ scattering.

Comparing Fig. 11 ($p\bar{p}\to W^-W^+$) with Fig. 6 ($d_L\bar{d}_R\to W^-W^+$ and $d_R\bar{d}_L\to W^-W^+$) we note that even in the final states with fixed vector boson polarizations the zero (still present in the $q\bar{q}$ case of Fig. 6) disappears due to summation over the two initial state polarizations, over u and d quarks and due to integration over the energy fractions available to the quarks and antiquarks which smear the positions of the energy dependent dips.

Since the cases $p\bar{p}\to Z^0\gamma$, $\to Z^0W$ and $\to ZZ$ are rather similar to the quark antiquark reactions shown in Figs. 4, 5, and 7, resp., they are not plotted here.

Certainly, our consideration is very simplified, since we use only valence quarks and neglect many smearing effects (e.g. parton transverse momenta and sea structure functions), however, it might be expected that the zero in the $\gamma W^\pm$ final state survives as a strong minimum in $p\bar{p}$ scattering with fixed position de-

termined by the gauge charge. Moreover, due to zeroes in various polarization states, strongly peaked angular distributions are predicted in $p\bar{p}\to Z^0\gamma$ and $\to Z^0W^-$. Their mechanisms in the $q\bar{q}$ scattering are discussed in the text:

they include
- zeroes at $\Theta=\pi/2$ ($\Theta=$scattering angle in the $q\bar{q}$ c.m.s.) for all $\hat{s}$
- zeroes moving with $\hat{s}$.

Acknowledgement. We thank Prof. J. Ranft for suggesting this investigation, many discussions and his stimulating interest in this work. Further thanks are to Dr. K. Gaemers, Prof. Ioffe, Dr. A. Kaidalov, and Prof. L. Okun.

References

1. K.O.Mikaelian, M.A.Samuel, D.Sahdev: Phys. Rev. Lett. **43**, 746 (1979)
2. R.W.Brown, D.Sahdev, K.O.Mikaelian: Phys. Rev. **D 20**, 1164 (1979)
3. K.J.F.Gaemers, G.J.Gounaris: Z. Phys. C – Particles and Fields **1**, 259 (1979)
4. W.Alles, Ch.Boyer, A.J.Buras: Nucl. Phys. **B 119**, 125 (1977) O.P.Sushkov, V.V.Flambaum, I.B.Kriplovitsch: Sovj. J. Nucl. Phys. **20**, 537 (1975)
5. J.D.Bjorken, M.C.Chen: Phys. Rev. **154**, 1337 (1967)
6. C.J.Goebel, F.Halzen, J.P.Leveille: Phys. Rev. **D 23**, 2682 (1981)
7. Zhu Dongpei: Phys. Rev. **D 22**, 2266 (1980)
8. R.W.Brown, K.O.Mikaelian: Phys. Rev. **D 19**, 922 (1979)
9. J.Kaur: Nucl. Phys. **B 128**, 219 (1977)
10. G.Ranft, J.Ranft: J. Phys. G (to appear)